Available online at www.eccomasproceedia.org
Eccomas Proceedia COMPDYN (2017) 4245-4258

ECCOMAS
Proceedia

COMPDYN 2017
6th ECCOMAS Thematic Conference on
Computational Methods in Structural Dynamics and Earthquake Engineering
M. Papadrakakis, M. Fragiadakis (eds.)
Rhodes Island, Greece, 15–17 June 2017

REINFORCED CONCRETE FRAMES STRENGTHENED BY TENSION-TIE ELEMENTS UNDER CYCLIC LOADING: A COMPUTATIONAL APPROACH

Angelos A. Liolios[1] **and Constantin E. Chalioris**[2]

[1] PhD Candidate
Democritus University of Thrace, Department of Civil Engineering,
Division of Structural Engineering, Xanthi 67100, GREECE
e-mail: aliolios@civil.duth.gr

[2] Associate Professor
Democritus University of Thrace, Department of Civil Engineering,
Division of Structural Engineering, Xanthi 67100, GREECE
e-mail: chaliori@civil.duth.gr

Keywords: Seismic Strengthening of RC Structures, X-braced Systems, Cable Elements, Tension-Ties, Shear-critical Frames, Computational Calibration Procedures.

Abstract. *An efficient numerical simulation of the seismic response of single-story single-span Reinforced Concrete (RC) frames strengthened using diagonal tension-tie elements is presented. The developed analysis is based, calibrated and verified on test results of bare and X-braced RC frames subjected to cyclic imposed lateral deformations described in a companion paper. The dimensional and the reinforcement configurations of the frames represent earlier RC frame structures that have been designed using old Code provisions without consideration of seismic design criteria and. The columns of the RC frames have shear-critical character due to the inadequate amount of stirrups provided and their low height-to-depth ratio (short columns). Therefore, an easy-to-apply strengthening technique using a pair of two steel crossed tension-ties (X-type bracing) is applied and examined. For the numerical simulation, the unilateral behavior of the cable elements that undertake only tension stresses is strictly taken into account. Comparisons between the analytical curves derived from the numerical simulation and the experimental ones from the cyclic tests showed a very good agreement.*

Peer-review under responsibility of the organizing committee of COMPDYN 2017.
doi: 10.7712/120117.5720.18195

1 INTRODUCTION

It is well known that many existing Reinforced Concrete (RC) frame buildings in seismically active countries have been designed and built according to past seismic Code standards. The provisions for reinforcement details of such old Codes are often not adequate for proper ductile seismic structural response with regards to modern Codes and structures. This holds especially for the shear-flexure behavior of existing RC members or/and structures under seismic excitations. A typical example of problematic local behavior is the case of the beam-column connections [1-6]. Concerning the global seismic response, a necessity for extensive strengthening often arises for such deficient RC frames and some of the well-known rehabilitation and upgrading techniques are widely applied [7-9].

A rather simple, low cost and efficient method for the global strengthening of RC frame structures against lateral induced earthquake loading is the use of steel cross X-bracings [10, 11]. An alternative technique that uses cable-like members as tension-ties instead of the common steel bracing has been proposed for seismic strengthening of RC frames [12, 13]. Cable restrainers have also been used for concrete and steel superstructure movement joints in bridges [14]. These cable elements can undertake severe tensional loads but when subjected to a compressive force they buckle and become slack and structurally ineffective under compression. Thus, the governing conditions take an equality form, as well as an inequality one, and the problem becomes nonlinear [15]. The mathematical solution of this problem can be achieved by the concept of variational and/or hemivariational inequalities [15, 16]. First approach of a computational procedure for single-story, single-span RC frame specimens has recently been developed by the authors [17].

Concerning the shear-flexure behavior of old RC structures under seismic actions a numerical procedure for shear-critical RC frames using layer-fiber micro-modeling in the sectional analysis has been presented [18]. Such micro-modeling methodologies are suitable for simulating simple laboratory RC frames of single-span and one or two stories [18, 19]. However, as emphasized by Fardis et al. [20], these methods seem to be very time-consuming and prohibiting for multi-story, multi-span RC frames, as is the case of the most common practical applications. On the other hand, special provisions for the shear-flexure behavior of existing RC members are included in recent intervention Code specifications that should be taken into account for assessment and retrofitting of older RC structures when their shear-dominated response has to be numerically estimated [21, 22,26-28].

This study presents a computational approach for the cyclic analysis under shear effects of existing RC frame structures strengthened by tension-tie elements. Two typical single-story single-span RC frames, one bare and one X-braced, are considered. The lateral cyclic behavior of these reference RC frames has been experimentally investigated and reported in a companion paper [23]. The dimensional and the reinforcement configurations of the examined frames represent typical RC frame structures that have been designed and constructed using old Code provisions without consideration of seismic design criteria and their columns have shear-critical character (inadequate amount of stirrups and low height-to-depth ratio). The shear effects are taken into account in the presented numerical procedure using the Ruaumoko code [24]. This computational procedure is verified by comparisons between the available test data and the herein computed results in terms of full cyclic lateral load versus displacement curves.

2 COMPUTATIONAL APPROACH

2.1 General principles of the numerical simulation

A double discretization in space and time is usually applied in Structural Dynamics [25]. First, the structural system is discretized in space by usual Finite Elements (FE). The macro-elements approach [8-10, 24] is preferable to the micro-elements one [18] for practical applications that concern multi-story multi-span RC frames. The most complex FE models are appropriate mainly for studying details and the simulation of tests on individual members or sub-assemblies due to their severe computational requirements and numerous input parameters [26]. Even fiber- models for distributed plasticity can be prohibitively complex for the simulation of entire realistic RC structures. Thus, a simple frame FE model that implements one-component model with concentrated plasticity at member ends is used herein as the best option for the practical non-linear seismic response analysis [24].

As concerns the cable-type steel elements modelling, pin-jointed bar elements are used. The unilateral behavior of these elements can in general include loosening, elastoplastic or/and elastoplastic-softening-fracturing and unloading-reloading effects. Concerning the full constitutive law of these steel elements and the usual general non-linearities concentrated at the two end critical regions (e.g. plasticity) of the RC structural members, these characteristics can be expressed mathematically by using concepts of convex and non-convex analysis [15, 16]. Thus, for the cable-elements behavior, the following relation holds:

$$s_i\ (d_i)\ \in\ \hat{\partial}\, SP_i(d_i) \tag{1}$$

where s_i and d_i are the (tensile) force (in [kN]) and the deformation (elongation) (in [m]), respectively, of the i cable element, $\hat{\partial}$ is the generalized gradient and SP_i is the super-potential function.

Incremental dynamic equilibrium for the assembled structural system with cables is expressed by the matrix relation:

$$M\,\Delta\ddot{\boldsymbol{u}} + C\,\Delta\dot{\boldsymbol{u}} + K_T\,\Delta u = -M\,\Delta\ddot{\boldsymbol{u}}_g + A\,\Delta s + \Delta p \tag{2}$$

where u(t) and p(t) are the displacement and the load time dependent vectors, respectively; $C(\dot{\boldsymbol{u}})$ and K_T (u) are the damping and the tangent stiffness matrix, respectively; A is a transformation matrix and u_g the ground seismic excitation. Dots over symbols denote derivatives with respect to time. By s(t) is denoted the cable stress vector satisfying the relation (1).

The above relations combined with the initial conditions consist the problem formulation, where, for given p and/or $\ddot{\boldsymbol{u}}_g$, the vectors u(t) and s(t) have to be computed.

2.2 Consideration of effects due to shear and to concrete cracking and confinement

Considering the shear effects, the RC structural elements are classified according to their shear span-to-depth ratio:

$$a_S = \frac{L_S}{d} = \frac{M}{Vd} \tag{3}$$

where $L_s = M/V$ is the shear length, M is the bending moment, V is the shear force and d is the section depth (height) of the examined member. In the case of RC frame columns or beams, the shear length L_s is equal to the half of the net height or span, respectively of the examined structural element [5, 20, 21].

Due to shear effects, the RC structural elements appear one of the following three behaviors depending on the shear span-to-depth ratio [9]:

1. Bending prevails and bending failure occurs before any shear failure, no matter if shear reinforcement exists or not if:

$$a_s = \frac{L_s}{d} = \frac{M}{Vd} \geq 7.0 \tag{4b}$$

2. Final flexural or shear failure mode depends on the provided shear reinforcement if:

$$2.0 \leq a_s = \frac{L_s}{d} = \frac{M}{Vd} \leq 7.0 \tag{4b}$$

3. Shear-critical short RC member is considered and special design procedure must be followed so that an explosive cleavage failure of the short column to be avoided if:

$$a_s = \frac{L_s}{d} = \frac{M}{Vd} \leq 2.0 \tag{4c}$$

Shear effects reduce the available plastic curvature φ_p of the critical sections of a RC member, as shown in Figure 1 of a typical moment versus curvature *(M - φ)* diagram [14]. So, the flexural ductile behavior is modified to a brittle one. The *M - φ* diagram of Figure 1 can be transformed to the shear force versus ductility diagram shown in Fig. 2 using $V = M / L_s$. According to the relation between the available shear strength capacity V_R and the required shear demand due to the flexural state, one of the three cases shown in Figure 2 can be realized. Thus, a shear failure and a so-caused reduction of the curvature ductility $\mu_\varphi = \varphi_u / \varphi_y$ can be eventually appeared or not.

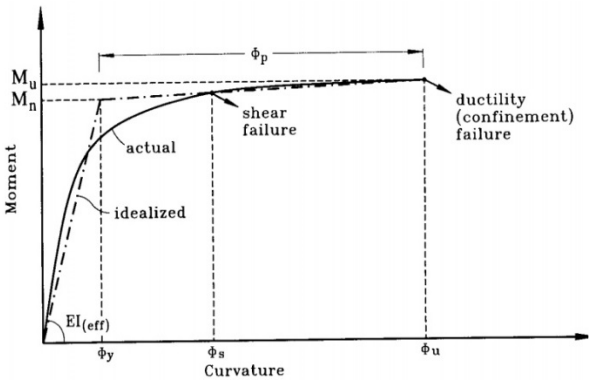

Fig.1. Reduction of the curvature and flexural ductility due to the shear failure [14]

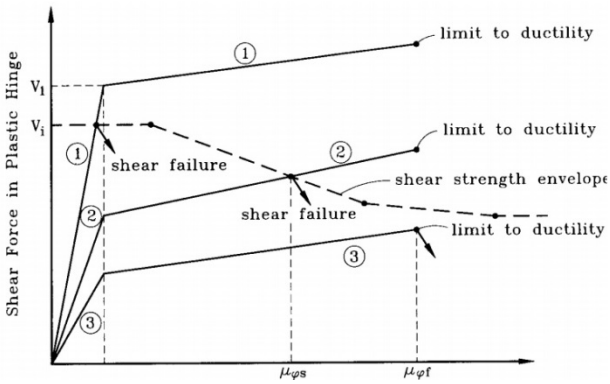

Fig.2. Available ductility under shear effects [14]

2.2.1. Effective flexural stiffness

During a seismic excitation the RC structural elements have a linear-elastic behavior until one or two of their critical end-regions enter to the yielding state, after concrete cracking, and therefore, plastic hinges are appeared [8,9, 20, 26]. The cracking effects on columns and beams are estimated by applying the guidelines of Eurocode 8, part 3 [21] and Greek Code of Interventions [22]. So, the effective flexural stiffness $E_c I_{eff}$ is given by the formula:

$$E_c I_{eff} = \frac{M_y \cdot L_s}{3 \cdot \theta_y} \tag{5}$$

where M_y and θ_y are the flexural moment and the chord rotation at yield, respectively, and L_s is the shear length corresponding to the member end.

2.2.2. Available cyclic shear strength

The available cyclic shear strength V_R of the examined member end is decreased with the incremental demand plastic chord rotation $\theta_{p,d}$ according to the following semi-empirical experimental expression [8, 21, 22, 26]:

$$V_R = \frac{1}{\gamma_{el}} \cdot \left[\frac{(h-x)\lambda_1}{2L_s} + (1-0.05\lambda_2) \cdot \left[0.16\lambda_3 (1-0.16\lambda_4) A_c \sqrt{f_{cm}/CF} + V_w \right] \right] \quad (6)$$

where γ_{el} is a safety factor that is taken equal to 1.15 for primary seismic structural elements (due to scattering of the experimental values) and is taken 1.00 for secondary seismic members; x is the compression zone depth (in m) known by the sectional analysis, CF is the Confidence Factor according to EC8-3 [21]; V_w is the contribution of the transverse reinforcement to the shear strength, taken as $V_w = \rho_w\, b_w\, z\, f_{yw,m}/CF$ for cross-section with web width b_w; ρ_w is the transverse reinforcement ratio: $\rho_w = (A_{sw}\, l_w)/(h_c\, b_c\, s_h)$; l_w is the total length of the stirrups, A_{sw} is the steel section area of the stirrup, h_c and b_c the dimensions of the confined core of the section and s_h is the centerline spacing of stirrups.

The λ parameters in Eq. (6) are considered as follows:

$$\lambda_1 = \min\left(N,\ 0.55A_c\, f_{cm}/CF\right) \quad (7a)$$

where N is the axial force (in MN), positive for compression and taken equal to zero when the axial force is tensional; $A_c = b_w\, d$; b_w is the width of compression zone and d is the depth of the tension reinforcement (in m); f_{cm} is the mean concrete compressive strength (in MPa).

$$\lambda_2 = \min\left(5,\ \mu_\Delta^p\right) \quad (7b)$$

where $\mu_\Delta^p = \theta_p/\theta_y$.

$$\lambda_3 = \max\left(0.5,\ 100\rho_{tot}\right) \quad (7c)$$

where ρ_{tot} is the total longitudinal reinforcement ratio (tensional, compression and intermediate bars).

$$\lambda_4 = \min\left(5,\ a_s\right) \quad (7d)$$

where a_s is the contemporary shear ratio.

2.2.3. Moment versus chord rotation diagram for the critical sections

In order to define the final elastic-plastic diagram of the Moment versus Chord Rotation (M - θ) of the critical section at the considered member end, it must be checked which type of failure precedes, the flexural or the shear failure [26-29]. Thus, using the calculated value of the shear strength V_R from Eq.(6), the moment $M_{u,v}$ at the critical section due to the V_R is estimated as

$$M_{u,v} = L_s \cdot V_R \quad (8)$$

When $M_{u,v} > M_y$, (M_y is the flexural yielding moment) then the flexural failure precedes the shear one and the final elastic-plastic of M - θ diagram of the examined member end is given by Figure 3(a). On the contrary, when $M_{u,v} < M_y$ then the shear failure precedes the flexural one and the final elastic-plastic M - θ diagram is given as the curve OABCD of Figure 3(b) [22, 26]. After the above check the final (corrected) values of M_y and θ_y are used in Eq. (5).

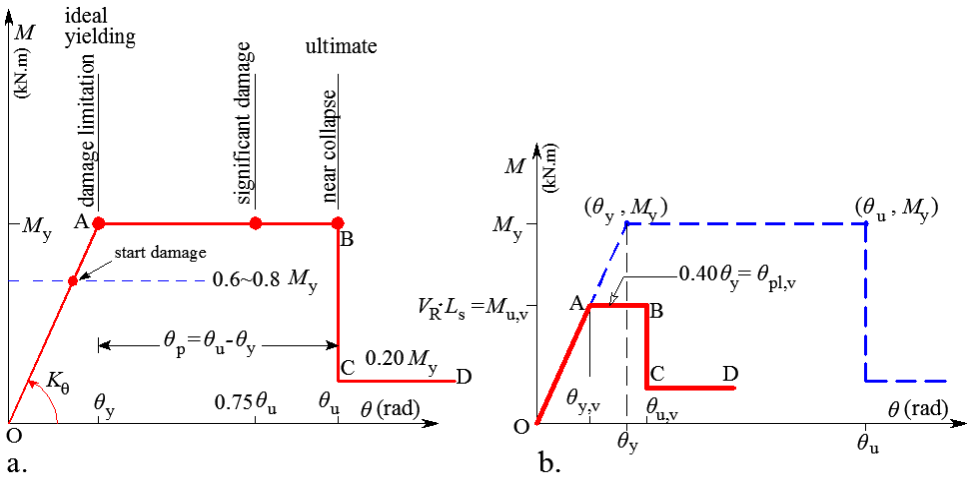

Fig.3. Moment versus chord rotation diagram for (a) ductile failure and (b) shear failure [26].

2.2.4. Effects of the concrete confinement for the critical sections

The ductility of RC structural elements is strongly influenced by the concrete confinement [5, 8, 9]. The stress versus strain diagram (σ - ε) of the confined concrete core can be calculated using a proper confined concrete model [21, 26]. Ductility also dependents on the ultimate strain $\varepsilon_{cu,c}$ of the extreme fiber in the compressive zone of the confined section and can be estimated by [9]:

$$\varepsilon_{cu,c} = \varepsilon_{cu} + 0.10 \cdot \alpha . \omega_{wd} \tag{9}$$

where ε_{cu} is the ultimate strain of unconfined concrete, ω_{wd} is the mechanical volumetric ratio of confining closed stirrups within the critical region and α is the confinement effectiveness factor of the core of the section, that is given as:

$$\alpha = \left(1 - \frac{s_h}{2b_c}\right) \cdot \left(1 - \frac{s_h}{2h_c}\right) \cdot \left(1 - \frac{\sum b_i^2}{6 \cdot b_c \cdot h_c}\right) \tag{10}$$

where s_h is the pure spacing of the provided transverse shear reinforcement (stirrups), b_1 is the centerline spacing of longitudinal bars laterally restrained by a stirrup corner along the perimeter of the cross-section, h_c and b_c is the dimension of confined core to the internal line of the external stirrup.

2.3 The software for the numerical simulation

For the numerical treatment of the problem, the structural analysis software Ruaumoko [24] is used. Ruaumoko is based on the FE method and can provide results for the RC buildings analysis [30] which concern, among others, the following critical parameters: Local or global structural damage, maximum displacements, inter-story drift ratios, development of plastic hinges and various response quantities, which allow the use of the incremental dynamic analysis (IDA) method [29] and the analysis of RC structures under multiple earthquakes [17]. For the consideration of inelastic shear behavior the SINA hysteresis model is implemented in Ruaumoko although it requires numerous input parameters. Generally, many additional input parameters for shear-effects are also required in such analyses for treating shear hinges.

Because of the aforementioned remarks and the reasons reported in the beginning of subsection 2.1, the software Ruaumoko is used. Moreover, in order to take into account shear and

other failure effects, the strength degradation model implemented in Ruaumoko and depicted in Figure 4 is used. “DUCT1”, “DUCT2” and “DUCT3” denote the ductility at which degradation begins, stops and at 0.01 initial strength, respectively. “RDUCT” is the residual strength as a fraction of the initial yield strength.

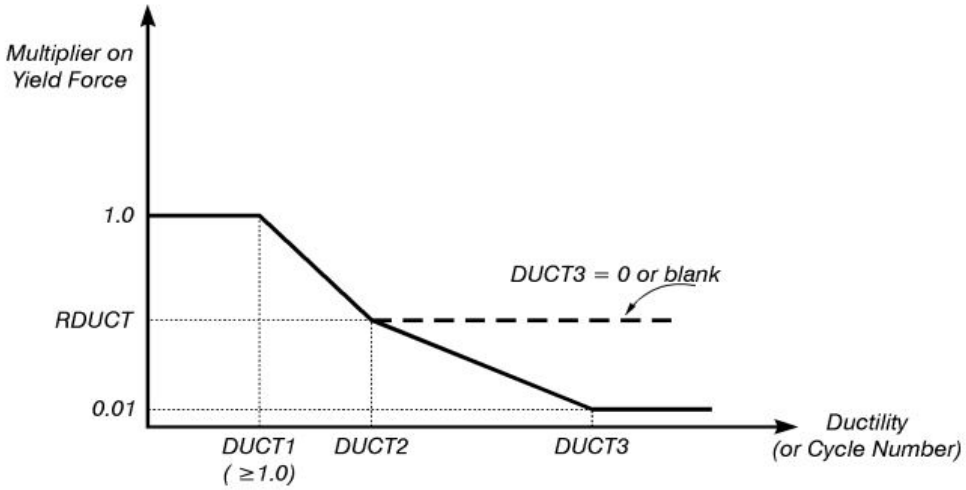

Fig.4. Strength degradation model implemented in Ruaumoko [24].

3 EXPERIMENTAL RESULTS FOR THE CALIBRATION OF THE COMPUTATIONAL APPROACH

The proposed numerical approach has already been used for the case of flexure-critical RC frames [17] using the available experimental results of typical flexural one-bay one-story RC moment-resistant frames, bare and strengthened with steel cross X-bracing [11]. Comparisons between the analytical curves derived from the numerical simulation and the experimental ones from these cyclic tests showed a very good agreement.

Here, for the calibration and verification of the presented numerical approach for the case of shear-critical RC frame structures the test results of relevant experiments reported in the companion paper [23] are used. Two models of RC frames have been investigated; the first is a bare frame without bracing (reference specimen), whereas the second one is strengthened with steel X-bracing of non-compression type (ties). The X-type bracing system consists of two steel rods installed as cable elements, connected to the RC frame through steel brackets. Dimensions and reinforcements of the examined frames represent typical RC frame of an old existing RC frame structure designed in accordance with past Code Standards in Greece.

A lateral additive cyclic quasi-static load was applied to the story beam in a displacement-controlled mode. The displacement history applied to both RC frames includes five different increasing loading steps at ± 1.0, ± 3.5, ± 12.0, ± 22.5 and ± 45.5 mm with two equal imposed cycles at each step. Details of the characteristics of the RC frame specimens, the X-bracing system, the experimental procedure and the test results can be found in [23].

The overall behavior of both specimens is presented in Figure 5 and compared in terms of load versus displacement hysteretic response. The X-braced RC frame (red dashed line) demonstrated increased load capacity and enhanced hysteretic performance with respect to the bare frame (blue continuous line). The bare RC frame failed due to the sudden shear diagonal cracking of the column, whereas in the X-braced one the shear failure has been prevented and two distinctive flexural plastic hinges have been formed in the beam. However, the X-braced frame

exhibited a rather sudden failure at both crossed tension-ties when the steel rods reached their ultimate strain limits.

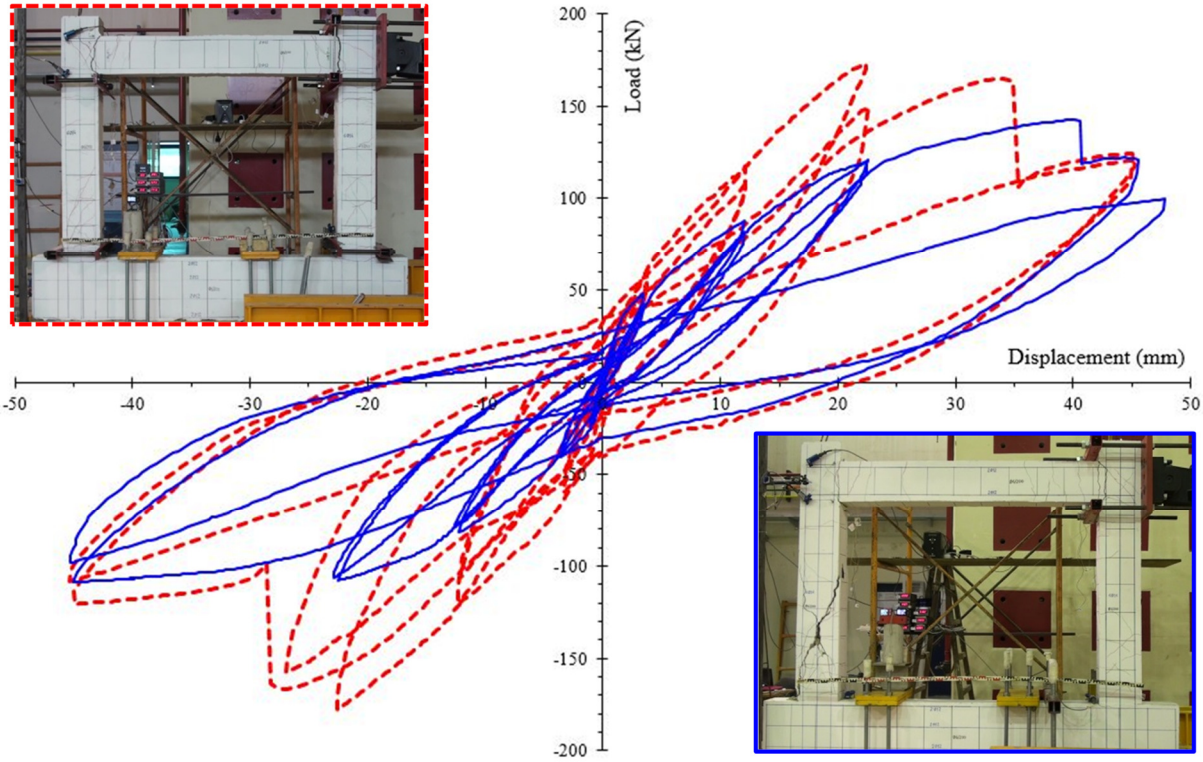

Fig.5. Comparative load versus displacement hysteretic diagram and failure modes of the X-braced frame (red dashed line) and the bare one (blue continuous line) [23]

4 COMPUTATIONAL SIMULATION OF THE TEST PROCEDURE

4.1 The Finite Element (FE) discretization of the RC frames

The FE models of the unbraced and braced RC frames are based on the test data. The columns and the beam are modeled using prismatic frame elements (Fig. 6). The imposed loading history has been simulated as displacement-controlled multiple earthquake excitation imposed on the top left node 3 of the frame (Fig. 6).

Nonlinearity at the two ends of RC members is idealized using one-component plastic hinge models, following the Takeda hysteresis rule. In order to check for shear-effects, the shear span-to-depth ratios of the RC members are computed according to Eq. (4) resulting to $a_s = 3.167$ for the beam and $a_s = 2.417$ for the columns. Thus, Eq. (4b) holds for each RC member since $2.0 \leq a_s \leq 7.0$ and the failure mode depends on the shear reinforcement of the member. The amount of the provided stirrups is rather low (∅6/200 mm) and their efficiency should be checked.

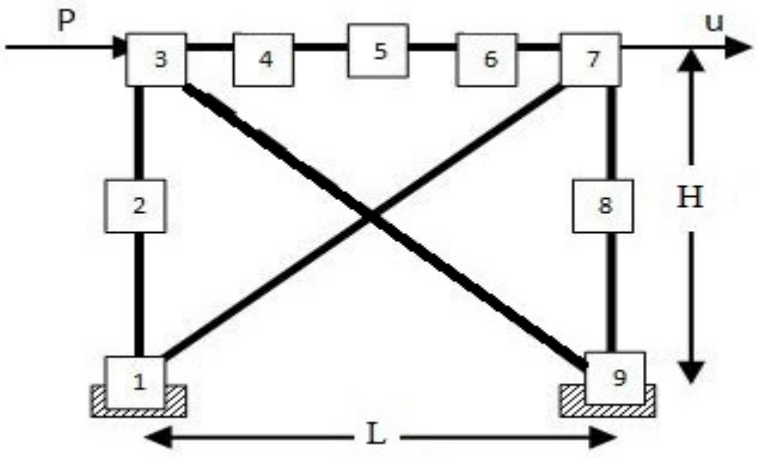

Fig.6. Finite element discretization of the simulated frame.

The absence of significant vertical gravity loads on the columns has as result the appearance of alternative axial forces (positive and negative, not only negative ones) as is the case of only compressive axial forces reported in the literature [11, 13, 19]. A preliminary simulation has given for these alternative axial forces the order results of the about values from -48 kN to +37 kN for the columns and from -67 kN to +55kN for the beam. Modelling of the two columns as well as of the beam is made by using the column-beam FE model of Ruaumoko [24]. The corresponding moment versus axial load (M - N) interaction curves computed by the section-analysis software RESPONSE-2000 [31] are shown in Fig. 7.

Based on the analysis of the critical sections insufficient confinement of the concrete core has first been detected. The spacing of the closed two-legged steel stirrups is 200 mm and therefore the confinement effectiveness factor α of the core of the sections is very low for the columns (α = 0.0495). Further, the mechanical volumetric ratio of the confining stirrups of the columns is $\omega_{wd} = 0.077 < 0.10$. Thus, Eq.(9) gives $\varepsilon_{cu,c} = \varepsilon_{cu}$ and the influence of the concrete - confinement to improve the RC member's ductility is minor and can be neglected.

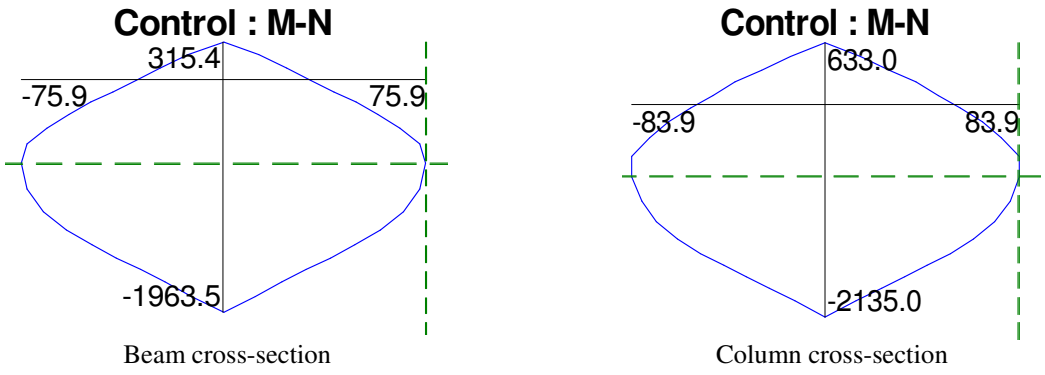

Fig.7. M - N interaction curves (in kNm and kN units) of the cross-sections of the members of the examined RC frames.

Concerning the available cyclic shear strength, V_R, computed by Eq.(6), it is about 5% lower than the developed required shear strength demand due to the flexure from -63 kN to +57 kN for the columns. So, shear effects according to Fig. 3(b) have been taken into account and slightly reduced values are used. The effective stiffness of the RC members is calculated by Eq.

(5) taking into account the shear effects. Moreover, the yield and the available ultimate ductility in plastic hinges are estimated for using the strength degradation model of Fig. 4.

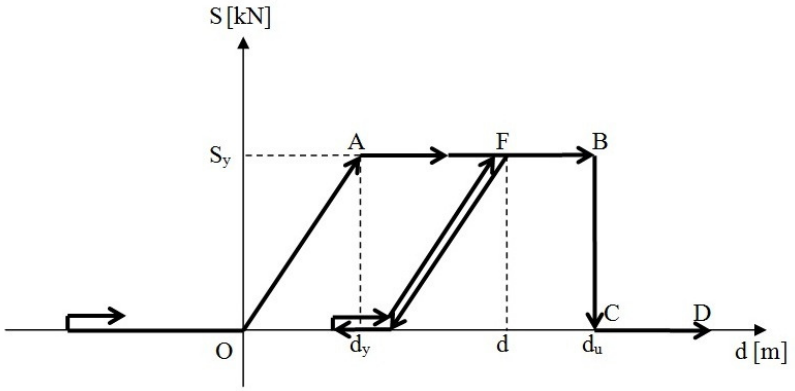

Fig.8. Constitutive law of the tension-tie elements.

For the X-bracing simulation spring-elements are used by applying the bilinear with slackness hysteresis rule of Ruaumoko [24]. These elements have cross-sectional area 1.0 cm^2 (corresponding to diameter ∅16 mm of the applied steel rods as tension-ties) and steel elasticity modulus 200 GPa. The cable constitutive law concerning the unilateral (slackness), hysteretic, fracturing, unloading-reloading behavior, has the simplified diagram *S-d* depicted in Fig. 8, where the ductility index is $\mu = d/d_y$. In the experimental procedure the failure strain of the crossed steel tension-ties has been measured for the ascending tie (member 1-7 in Fig. 6) and for the descending tie (member 3-9 in Fig. 6). Taking into account these failure limits the corresponding available ultimate ductility for each tie are computed and used for the strength degradation model of Fig. 4.

4.2 Representative results of the numerical simulation

The computationally derived diagrams of the load, P, versus top displacement, u, hysteretic behavioral curves for the unbraced (bare) frame and the X-braced frame are shown in Fig. 9 and Fig.10, respectively, in comparison with the experimentally obtained ones. From these comparisons it is indicated that the computed results are in very good agreement with the experimental data curves.

5 CONCLUDING REMARKS

A computational approach for the lateral cyclic inelastic behavior of single-story single-span RC frames under shear effects, which are strengthened using X-type steel tension-ties has been presented. Emphasis is given to the dimensional and reinforcement configuration of old RC frame structures that have been designed and constructed using past Code provisions without proper seismic requirements and appear shear character problems due to the lack of adequate stirrups and the short shear length in the columns, and therefore a shear-dominated behavior is expected.

The developed approach has been calibrated and verified by simulating available experimental results presented in a companion paper. Comparisons between experimental and computed results show that the presented computational approach could effectively be used for the seismic assessment and the strengthening of existing shear-critical RC frame structures by X-type tension-tie or cable elements.

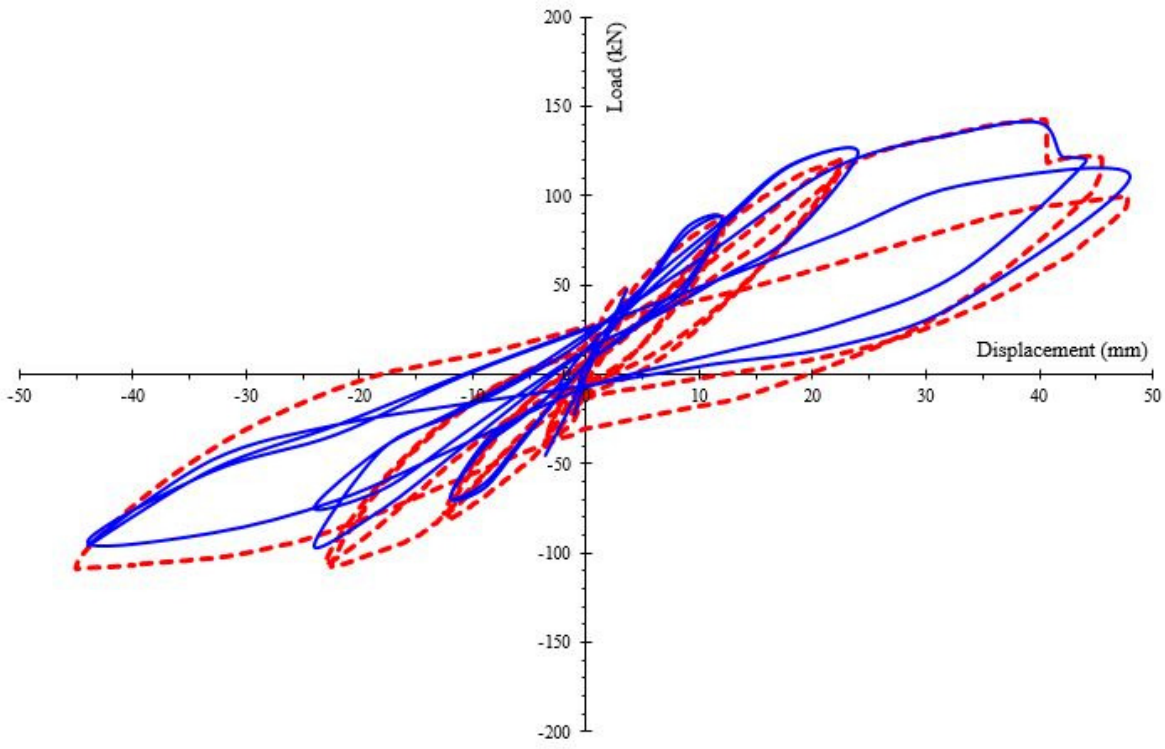

Fig.9. Unbraced (bare) RC frame: Computational (*continuous blue lines*) versus experimental (*dashed red lines*) hysteretic response.

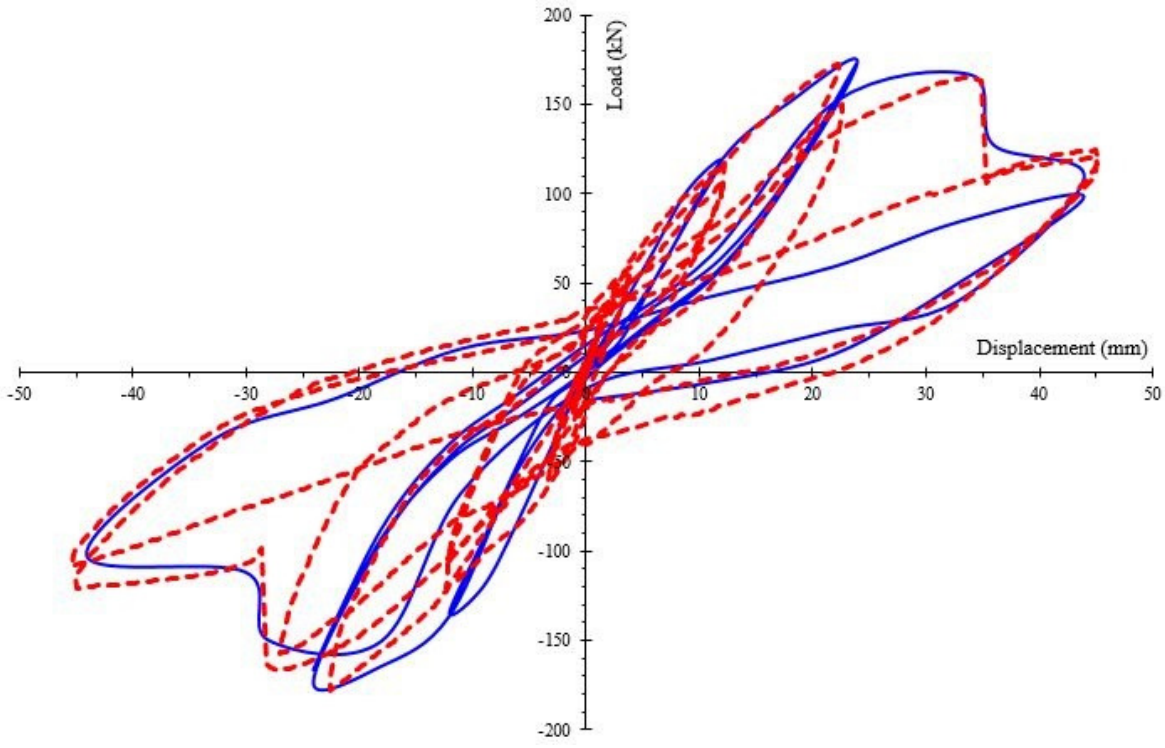

Fig.10. Braced (X-strengthened) RC frame: Computational (*continuous blue lines*) versus experimental (*dashed red lines*) hysteretic response.

REFERENCES

[1] Tsonos, A.-D.G. (2007). *Cyclic load behavior of RC beam-column subassemblages of modern structures*. ACI Structural Journal, 104(4), 468-478.

[2] Chalioris, C.E., Favvata, M.J. and Karayannis, C.G. (2008). *Reinforced concrete beam–column joints with crossed inclined bars under cyclic deformations*. Earthquake Engineering & Structural Dynamics, 37(6), 881-897.

[3] Favvata, M.J., Izzuddin, B.A. and Karayannis, C.G. (2008). *Modelling exterior beam-column joints for seismic analysis of RC frame structures*. Earthquake Engineering & Structural Dynamics, 37(13), 1527-1548.

[4] Karayannis, C.G. Favvata, M.J. and Kakaletsis, D.J. (2011). *Seismic behaviour of infilled and pilotis RC frame structures with beam–column joint degradation effect*. Engineering Structures, 33(10), 2821-2831.

[5] Karayannis, C. G. (2014), *Seismic design of reinforced concrete structures*. (in greek). Sofia Publications, Thessaloniki, Greece.

[6] Kalogeropoulos, G.I., Tsonos, A.-D.G., Konstandinidis, D. and Tsetines, S. (2016). *Pre-earthquake and post-earthquake retrofitting of poorly detailed exterior RC beam-to-column joints*. Engineering Structures, 109, 1-15.

[7] Dritsos, S.E., (2001). *Repair and strengthening of reinforced concrete structures* (in greek). University of Patras, Greece.

[8] Fardis, M.N., (2009). *Seismic design, assessment and retrofitting of concrete buildings: based on EN-Eurocode 8*. Springer, Berlin.

[9] Penelis, G. and Penelis, Greg. (2014). *Concrete buildings in seismic regions*. CRC Press, Taylor & Francis Ltd.

[10] Antonopoulos, T.A. and Anagnostopoulos, S.A. (2013). *Improving the seismic performance of existing old pilotis type buildings by strengthening only the ground story*, In: M. Papadrakakis, V. Papadopoulos & V. Plevris (eds.), *COMPDYN 2013, ECCOMAS: Thematic Conference on Computational Methods in Structural Dynamics and Earthquake Engineering*, Kos Island, Greece, 12–14 June 2013.

[11] Massumi, A. and Absalan, M. (2013). *Interaction between bracing system and moment resisting frame in braced RC frames.* Archives of Civil and Mechanical Engineering, 13(2), 260-268.

[12] Markogiannaki, O. and Tegos, I. (2011). *Strengthening of a multistory R/C building under lateral loading by utilizing ties.* Applied Mechanics and Materials, 82, 559-564.

[13] Lee, K. S. (2015). *An experimental study on non-compression X-bracing systems using carbon fiber composite cable for seismic strengthening of RC buildings*. Polymers, 7(9), 1716-1731.

[14] Priestley, M.J.N., Seible, F.C. and Calvi, G.G.M. (1996). *Seismic design and retrofit of bridges*. John Wiley & Sons, Inc.

[15] Panagiotopoulos, P.D. (1993). *Hemivariational inequalities. Applications in mechanics and engineering*. Springer-Verlag, Berlin, New York, (1993).

[16] Mistakidis, E.S. and Stavroulakis, G.E. (1998). *Nonconvex optimization in mechanics. Smooth and nonsmooth algorithmes, heuristic and engineering applications*. Kluwer, London.

[17] Liolios, A. and Chalioris, C.E. (2015). *Reinforced concrete frames strengthened by cable elements under multiple earthquakes: A computational approach simulating experimental results*. In: *Proceedings of 8th GRACM International Congress on Computational Mechanics,* pp. 12-15, *Volos, Greece*.

[18] Güner, S. and Vecchio, F.J. (2010). *Analysis of shear-critical reinforced concrete plane frame elements under cyclic loading*. Journal of Structural Engineering, 137(8), 834-843.

[19] Karalis, A. A., Georgiadi-Stefanidi, K. A., Salonikios, T. N., Stylianidis, K. C., & Mistakidis, E. S. (2011). *Experimental and numerical study of the behaviour of high dissipation metallic devices for the strengthening of existing structures*. In: M. Papadrakakis et al, (eds.), *Proceedings of COMPDYN 2011, ECCOMAS: Thematic Conference on Computational Methods in Structural Dynamics and Earthquake Engineering,* Corfu, Greece, 26–28 May 2011.

[20] Fardis, M. N., Carvalho, E. C., Fajfar, P. and Pecker, A. (2015). *Seismic design of concrete buildings to Eurocode 8.* CRC Press, Taylor and Francis Group, New York.

[21] EC8-3, Eurocode 8 (CEN 2004). *Design of structures for earthquake resistance, Part 3: Assessment and retrofitting of buildings*, (EC8-part3), EN 1998-3, Brussels.

[22] KAN.EPE (2013). *Greek Code of Interventions*. Team for development of code of interventions on reinforced concrete buildings, Harmonization team of code of interventions to Eurocodes: Council of Europe, European Centre on Prevention and Forecasting of Earthquakes (E.C.P.F.E.), Earthquake Planning and Protection Organization (E.P.P.O.), Athens.

[23] Liolios A., Efthymiopoulos P., Mergoupis T., Rizavas V. and Chalioris C. E. (2017). *Reinforced concrete frames strengthened by tension-tie elements under cyclic loading: Experimental investigation*. In: Papadrakakis, M. et al (eds.), Proceedings of COMPDYN 2017: *Computational Methods in Structural Dynamics and Earthquake Engineering, paper C18197*, 15-17 June 2017, Rhodes Island, Greece

[24] Carr, A.J. (2008). *RUAUMOKO - Inelastic Dynamic Analysis Program*. Department of Civil Engineering, University of Canterbury, Christchurch, New Zealand.

[25] Chopra, A.K., (2007). *Dynamics of Structures: Theory and Applications to Earthquake Engineering*, Pearson Prentice Hall, New York.

[26] Makarios T. (2013), "*Modelling of characteristics of inelastic members of reinforced concrete structures in seismic nonlinear analysis*", Ch. 1, pp. 1-41, In: G. Padovani and M. Occhino (Editors): *Focus on Nonlinear Analysis Research*, Nova Publishers, New York.

[27] Psycharis, I. N. (2015), *Antiseismic Design with Performance Levels*. Postgrad. Lecture Notes (in greek), National Technical University of Athens, Dept. Civil Engineering.

[28] Mergos, P.E. & Kappos, A. J. (2013). *Damage Analysis of Reinforced Concrete Structures with Substandard Detailing.* In: M. Papadrakakis, M. Fragiadakis & V. Plevris (Eds.), *Computational methods in earthquake engineering: Volume 2.* Computational Methods in Applied Sciences, 30. (pp. 149-176). Springer. ISBN 978-94-007-6572-6.

[29] Vamvatsikos, D. and Cornell, C.A., (2002). *Incremental dynamic analysis*. Earthquake Engineering and Structural Dynamics, vol. 31, 491–514.

[30] Paulay T. and Priestley, M.J.N. (1992), "*Seismic design of reinforced concrete and masonry buildings*". Wiley, New York.

[31] Bentz, E. C. (2000). *Sectional analysis of reinforced concrete members, (RESPONSE-2000).* PhD thesis, Dept. Civil Engineering, University of Toronto.